Int. J. Heat Mass Transfer. Vol. 19, pp. 931–941. Pergamon Press 1976. Printed in Great Britain

BUBBLE GROWTH RATES IN NUCLEATE BOILING OF AQUEOUS BINARY SYSTEMS AT SUBATMOSPHERIC PRESSURES

S. J. D. VAN STRALEN, W. M. SLUYTER and R. COLE†
Transportphysics Section, Eindhoven University of Technology, Eindhoven, Netherlands

(*Received* 12 *September* 1975)

Abstract—The growth rate of vapour bubbles has been investigated experimentally in the following binary systems with a more volatile organic component: water–ethanol (up to 31 wt% ethanol, at pressures between 4.08 and 6.65 kPa, the Jakob number varying from 1989 to 1075), water–1-butanol (up to 2.4 wt% 1-butanol, at pressures between 3.60 and 4.08 kPa, the Jakob number varying from 2760 to 1989), and water–2-butanone (up to 15 wt% 2-butanone, at pressures between 7.31 and 9.07 kPa, the Jakob number varying from 1519 to 683).

Experimental bubble growth is in quantitative agreement with the van Stralen *et al.* theory [1], which combines the initially dominating Rayleigh solution with a (heat and mass) diffusion-type solution for the contributions to advanced bubble growth due to both the relaxation microlayer (around the bubble dome) and the evaporation microlayer (beneath the bubble).

The slowing-down effect of mass diffusion on advanced bubble growth in mixtures occurs only in the system water–2-butanone. The contribution of the evaporation microlayer is negligible (at any pressure) for mixtures with a low concentration of the more volatile component, in which mass diffusion limits advanced growth considerably.

NOMENCLATURE

a, liquid thermal diffusivity [m^2/s];
b^*, dimensionless bubble growth parameter during adherence;
c, liquid specific heat at constant pressure [J/kgK];
C_1, asymptotic bubble growth constant [$m/s^{\frac{1}{2}}K$];
D, mass diffusivity of more volatile component in less volatile component [m^2/s];
e, 2.718..., base of natural logarithms;
G, vaporized mass fraction;
Ja, $= (\rho_1 c/\rho_2 l)\theta_0$, Jakob number for superheated liquid;
k, liquid thermal conductivity [W/mK];
K, equilibrium constant of more volatile component in binary mixture (ratio of mass fractions in vapour and liquid);
l, latent heat of vaporization [J/kg];
p, ambient pressure [$Pa = N/m^2 = kg/ms^2$];
Pr, $= v/a$, liquid Prandtl number;
q, heat flux density [W/m^2];
R, = equivalent spherical bubble radius [m];
$R(t_1)$, = equivalent spherical bubble departure radius [m];
R_1, equivalent bubble radius according to modified Rayleigh solution [m];
R_2, equivalent bubble radius according to total diffusion (combined evaporation and relaxation microlayer) solution [m];
R_c^*, radius of contact area between bubble and heating surface [m];
t, bubble growth time during adherence [s];
t_1, bubble departure time [s];
t_c, instant of maximum contact radius [s];
T, absolute boiling temperature [K];
$T(x)$, absolute boiling temperature of liquid at bubble boundary in binary mixture [K];
$T(x_0)$, absolute boiling temperature of original liquid in binary mixture [K];
ΔT, $= T(x) - T(x_0)$, increase in temperature of liquid at bubble boundary with respect to original liquid [K];
x, $= x_0/\{1+(K-1)G\}$, mass fraction of more volatile component in liquid at bubble boundary in binary mixture;
x_0, mass fraction of more volatile component in original binary mixture;
y, mass fraction of more volatile component in vapour.

Greek symbols

Θ_0, superheating of heating surface or (for free bubbles) uniform superheating of liquid [K];
v, liquid kinematic viscosity [m^2/s];
ρ_1, liquid density [kg/m^3];
ρ_2, saturated vapour density [kg/m^3].

Subscripts

m, binary mixture;
max, nucleate boiling peak flux;
p, pure liquid;
w, heating surface.

†Department of Chemical Engineering, Clarkson College of Technology, Potsdam, NY 13676, U.S.A.

1. PREVIOUS INVESTIGATIONS

VAN STRALEN *et al.* [1] developed a theoretical model for the growth of vapour bubbles, which combines the effect of both relaxation microlayer (around the lower part of the bubble boundary) and evaporation-microlayer (between bubble and heating wall) with the Rayleigh solution. The decrease of the superheating enthalpy of both microlayers during bubble growth is taken into account.

Van Stralen *et al.* [2] investigated experimentally the growth rate of vapour bubbles up to departure in *water* boiling at pressures varying from 26.7 to 2.04 kPa, the corresponding Jakob number increasing from 108 to 2689. The experimental bubble growth rates are in quantitative agreement with the theoretical model [1]. Cole and van Stralen [3] showed, that this is also the case for previous results of Stewart and Cole [4] on *water* boiling at a pressure of 4.9 kPa, the Jakob number varying from 955 to 1112.

2. SCOPE OF THE PRESENT INVESTIGATIONS

The experimental investigations on bubble growth rates have been extended now to the following "positive" aqueous binary systems with a more volatile (organic) component: *water–ethanol* (up to a mass fraction of 0.31 and pressures ranging from 4.08 to 6.65 kPa, the corresponding Jakob number varying from 1989 to 1075), *water–1-butanol* (up to a mass fraction of 0.024 and pressures ranging from 3.60 to 4.08 kPa, the corresponding Jakob number varying from 2760 to 1989) and *water–2-butanone* (up to a mass fraction of 0.15 and pressures ranging from 7.31 to 9.07 kPa, the Jakob number varying from 1519 to 683).

The investigations are limited to relatively small concentrations of the organic component as advanced isobaric (heat and mass) diffusion-controlled bubble growth is expected to show a minimum in this range. Contrarily, initial (isothermal) bubble growth is governed by liquid inertia, i.e. the bubble is blown up according to the Rayleigh solution. Hence, initial growth is a priori expected to be independent of concentration.

3. FINAL BUBBLE GROWTH EQUATIONS

3.1. *General expression for the equivalent bubble radius in unary and binary systems*

According to Cooper and Vijuk [5], bubble growth during the transition stage (between isothermal and isobaric growth) is approximated by the following semi-empirical expression:

$$R(t) = \frac{R_1(t)R_2(t)}{R_1(t)+R_2(t)}. \tag{1}$$

In the case of non-uniform liquid superheating (at a heating wall), van Stralen *et al.* [1] showed, that initially the modified Rayleigh solution governs bubble growth:

$$R_1(t) = 0.816\left\{\frac{\rho_2 l\Theta_0 \exp -(t/t_1)^{\frac{1}{2}}}{\rho_1 T}\right\}^{\frac{1}{2}} t$$

$$= 0.816\left\{\frac{c}{T}\exp -(t/t_1)^{\frac{1}{2}}\right\}^{\frac{1}{2}} (Ja)^{-\frac{1}{2}}\Theta_0 t. \tag{2}$$

Initially, the presence of the evaporation microlayer has no effect on bubble growth. Advanced bubble growth in mixtures is determined by combined heat and mass diffusion (of the more volatile component) towards the bubble boundary:

$$R_{2,m} = \frac{C_{1,m}}{C_{1,p}}\left(1.954b^* + 0.373\frac{C_{1,m}}{C_{1,p}}Pr^{-\frac{1}{3}}\right)$$

$$\times \{\exp -(t/t_1)^{\frac{1}{2}}\} Ja(at)^{\frac{1}{2}}. \tag{3}$$

The first term on the RHS of equation (3) is due to evaporation at the lower part of the bubble boundary (the contribution to bubble growth of the "relaxation microlayer"), the second term is due to heat transmission through the thin (liquid) "evaporation microlayer", which is formed between bubble and heating wall. The effect of the superheating of the bulk liquid has been neglected in (3), as generally this superheating is of the order of 0.1–1 K in nucleate boiling.

In the derivation of equations (2) and (3), a uniform vapour temperature and thermodynamic equilibrium at the bubble boundary is assumed, in which case the Clapeyron equation is valid for unary systems (one-component systems). It follows from equations (2) and (3), respectively, that $R_1 \sim p^{\frac{1}{2}}$ and $R_2 \sim p^{-2}$ (at low pressures). According to equation (1), R_1 governs initial bubble growth, especially at low (subatmospheric) pressures ($p \to 0$). This is confirmed by numerical computer calculations carried out by Zijl [6], showing that the superheating of the bubble boundary decreases then very slowly from the initial value Θ_0 to zero. The same result follows from a simple physical model, which is based on the concept of initial heat removal from the bubble boundary with a constant heat flux density: $q = \rho_2 l\dot{R}_1(t) =$ constant, cf. equation (2); the surrounding liquid is considered to be a semi-infinite body, cf. [7]. The decrease of the superheating of the bubble boundary is thus proportional to $\rho_2^{\frac{1}{2}} \sim p^{\frac{1}{2}}$, and vanishes as $p \to 0$. Consequently, "Rayleigh bubbles" have been observed in water at pressures below 3 kPa [2].

The bubble growth constant $C_{1,m}$ for asymptotic diffusion-controlled growth of a spherically symmetric free bubble in an initially uniformly superheated infinite liquid is given by the following expression:

$$C_{1,m} = \left(\frac{12}{\pi}\right)^{\frac{1}{2}} \frac{a^{\frac{1}{2}}}{(\rho_2/\rho_1)\{(l/c)+(a/D)^{\frac{1}{2}}\Delta T/G\}}. \tag{4}$$

In case of an unary system (and in azeotropic mixtures), the increase in dewpoint of the vapour in a bubble $\Delta T = 0$, whence $C_{1,m} = C_{1,p}$, with

$$C_{1,p} = \left(\frac{12}{\pi}a\right)^{\frac{1}{2}} \frac{Ja}{\Theta_0} = \left(\frac{12}{\pi}\right)^{\frac{1}{2}} \frac{(k\rho_1 c)^{\frac{1}{2}}}{\rho_2 l}. \tag{5}$$

According to equation (4), $C_{1,m}$ shows a minimum at the (small) fraction x_0 of the more volatile component, at which $\Delta T/G$ is maximal; i.e. asymptotic bubble growth is slowed down maximally then. The reader is referred to the Appendix for the derivation of equation (16), which expresses $C_{1,m}/C_{1,p}$ into material constants.

3.2. *Determination of the bubble growth parameter*

The numerical value of the bubble growth parameter b^* (which denotes the relative height of the relaxation microlayer around the bubble boundary) is determined by taking $t = t_1$, the departure time, in equations (1)–(3). Actually, the theoretical model by van Stralen *et al.* [1] is able to predict t_1, but (at low pressures) the departure radius $R(t_1)$ has to be derived from experiment. Contrarily, at higher pressures, $b^* = 1$, and the theoretical predictions include the departure radius. A complication to predict b^* theoretically at low (subatmospheric) pressures arises from the fact, that the initial thickness of the relaxation microlayer may exceed the expected value. This is caused by a larger thickness of the thermal liquid boundary layer, at the heating wall, which may extend to large values due to heat conduction. This influence has been incorporated in the Mikic, Rohsenow and Griffith model [8]; however, the evaporation microlayer has not been included by these authors, cf. [1, 2].

For numerical calculations, the theoretical $R(t_1)$ is taken equal to the experimental value, resulting in the following expression for the bubble growth parameter:

$$b^* = 1.391\left(\frac{C_{1,p}}{C_{1,m}}\right)\frac{R_2(t_1)}{Ja(at_1)^{\frac{1}{2}}} - 0.191\left(\frac{C_{1,m}}{C_{1,p}}\right)Pr^{-\frac{1}{3}}. \quad (6)$$

Bubble growth up to departure is given by equations (1)–(3) by inserting the derived value of b^* into equation (3).

The departure radius $R(t_1)$ follows from equation (1):

$$R(t_1) = \frac{R_1(t_1)R_2(t_1)}{R_1(t_1)+R_2(t_1)} \quad (7)$$

One has according to the modified Rayleigh equation (2):

$$R_1(t_1) = 0.495\left(\frac{\rho_2 l}{\rho_1 T}\Theta_0\right)^{\frac{1}{2}} t_1, \quad (8)$$

and according to equation (3) for the total diffusion equation:

$$R_{2,m}(t_1) = \frac{C_{1,m}}{C_{1,p}}\left(0.719b^* + 0.137\frac{C_{1,m}}{C_{1,p}}Pr^{-\frac{1}{3}}\right)Ja(at_1)^{\frac{1}{2}} \quad (9)$$

Substitution of $R_1(t_1)$ from (8) into (7) yields $R_2(t_1)$ and, consequently, b^* follows from (6).

3.3. *Effect of Jakob number on bubble growth*

Obviously, both initial and advanced bubble growth are governed by the value of the Jakob number, cf. equations (1)–(3), i.e. the most influential parameter is ρ_2, the density of saturated vapour. According to the ideal gas law, which is valid accurately for the vapour at subatmospheric pressures, $Ja \sim \rho_2^{-1} \sim p^{-1}$.

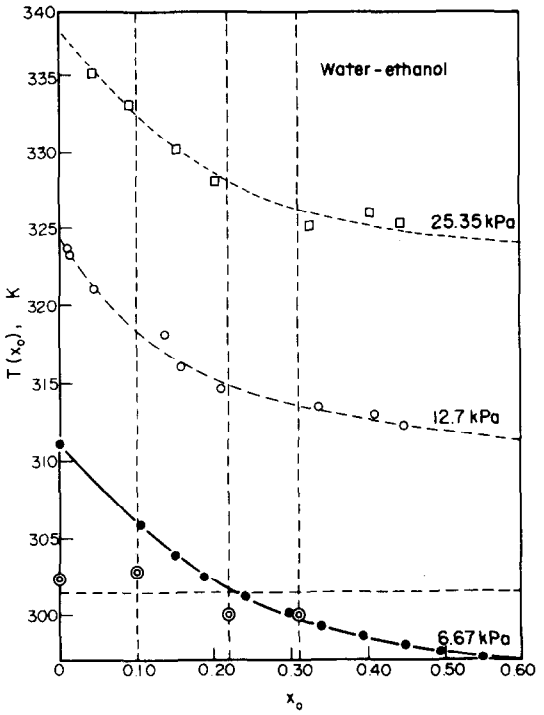

FIG. 1. Water–ethanol. Experimental equilibrium boiling point curves at various subatmospheric pressures [9]. Dotted (vertical and horizontal) lines and figures, ⊙, correspond with experiments on bubble growth (Figs. 3 and 4). Boiling point curves tally by a vertical displacement.

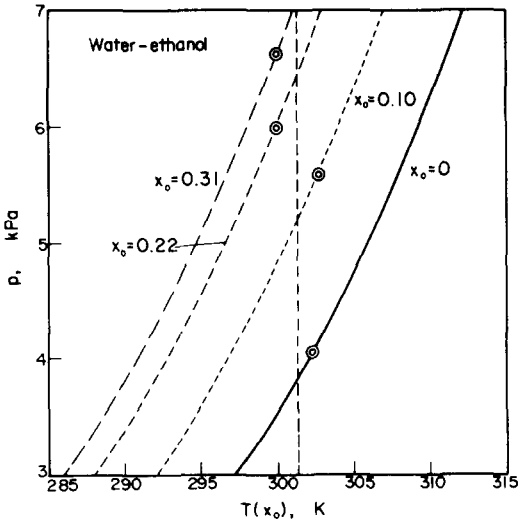

FIG. 2. Water–ethanol. (p, T)-diagram for various liquid compositions, cf. Fig. 1. Dotted vertical line and figures, ⊙, correspond with experiments on bubble growth (Figs. 3 and 4).

4. EXPERIMENTAL CONDITIONS AND EVALUATION OF RESULTS

4.1. *Experimental setup*

The experimental setup and high speed cinematographic techniques are described in [2].

4.2. *Equilibrium data at subatmospheric pressures*

Equilibrium data for the system water–ethanol at subatmospheric pressures are taken from literature [9]. For the other investigated systems, extrapolations had to be made from data at atmospheric and elevated pressures, cf. the Appendix.

Boiling-point curves for water–ethanol at several subatmospheric pressures are shown in Fig. 1. The (p, T)-curves, represented in Fig. 2, are derived from Fig. 1. The curve for $x_0 = 0$ (water) is the (p, T)-curve according to the Clapeyron equation. The curves shown in Fig. 1 tally if they are shifted vertically over a suitable constant temperature difference, which is independent of x_0. It follows from the experimental equilibrium data taken from [9], that the slope of the (p, T)-curves for different (constant) values of x_0 is independent of x_0 at arbitrary constant (low) pressure, i.e. the curve for any $x_0 (\leqslant 0.31)$ follows by a horizontal translation of the curve for $x_0 = 0$ (water).

4.3. *The Clapeyron-equation for binary systems*

This result can also be derived theoretically. In case of regular solutions (which have the same entropy of mixing as an ideal solution, but an enthalpy of mixing, which differs from zero), the partial vapour pressure curve of the components obey the Clapeyron-equation [10, 11]. For the system water–ethanol the specific enthalpy of mixing [12] has the following numerical values (which are obviously negligible in comparison to the specific enthalpy of vaporization $l \approx 2 \times 10^3$ kJ/kg): (i) at a constant temperature of 353 K: 0 at $x_0 = 0.35$, 4.2 kJ/kg (maximum) at $x_0 = 0.17$ and -13.4 kJ/kg (minimum) at $x_0 = 0.70$; (ii) at 323 K: 0 at $x_0 = 0.70$, 20 kJ/kg (maximum) at $x_0 = 0.26$ and -3.6 kJ/kg (minimum) at $x_0 = 0.82$; (iii) at 273 K the minimum has disappeared and a maximum of 51 kJ/kg occurs at $x_0 = 0.30$.

Consequently, as an approximation, the Clapeyron-equation can also be applied to the investigated binary mixtures. One has at constant (low) pressure:

$$(\rho_2 l)_m = T_m \left(\frac{dp}{dT}\right)_m \approx T_p \left(\frac{dp}{dT}\right)_p = (\rho_2 l)_p. \qquad (10)$$

Equation (10) is useful in the common case, that numerical values of $\rho_{2,m}$ and l_m are not known in literature. The values of these material constants for mixtures can also be estimated by interpolation of the corresponding values for the pure components, e.g. for water–2-butanone (in the investigated range: $x_0 \leqslant 0.15$): $(\rho_2 l)_m \approx (\rho_2 l)_p$, as for water at atmospheric pressure and boiling point (373 K): $\rho_{2,p} = 0.598$ kg/m^3 and $l_p = 2256$ kJ/kg and for 2-butanone (at 353 K): $\rho_{2,p} = 2.49$ kg/m^3 and $l_p = 433$ kJ/kg. The ratio of the product $(\rho_2 l)_p$ in the pure components amounts thus to $1349/1078 = 1.25$. Hence (at constant pressure) for $x_0 \leqslant 0.15$: $(\rho_2 l)_m \approx (\rho_2 l)_p$, the value in water. According to equations (1)–(3), the product $\rho_2 l = \rho_1 c \Theta_0 / Ja$ is the most influential bubble growth parameter, cf. Section 3.3. The separate effect of $\rho_{2,m} > \rho_{2,p}$ on the second term in the denominator of the RHS of equation (4) has been neglected in the numerical calculations.

4.4. *The Jakob number*

In the evaluation of the theoretical equations $(\rho_2 l)_m = (\rho_2 l)_p$ (and Ja) have been taken at the operating pressure, both in the Rayleigh solution, equation (2), and in the total diffusion solution, equation (3). Actually, initial evaporation occurs at the temperature $T + \Theta_0$. However, the effect of this on the theoretical bubble growth curves is shown to be negligible or small, the latter during initial growth, where $R(t) \to R_1(t)$ as $t \to 0$; nevertheless, the value of the Jakob number is affected seriously. The other material constants are taken at T, with exception of the Prandtl number Pr, which is taken at $T + \frac{1}{2}\Theta_0$.

4.5. *Experiments at constant saturation temperature*

At constant pressure, the boiling point in the region of total miscibility decreases by adding a more volatile component to water (cf. e.g. Figs. 1 and 2). For convenience, the experiments have been carried out at a nearly constant saturation temperature, which exceeds room temperature only with a few degrees kelvin. This procedure results in a higher saturation pressure in the mixtures in comparison to water.

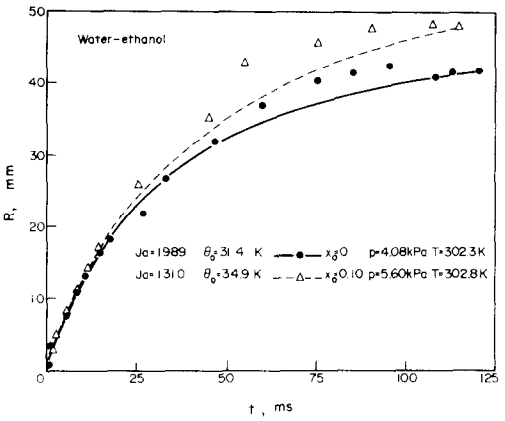

FIG. 3. Water–ethanol. Experimental bubble growth data up to departure in comparison with theory, [1] and equations (1)–(9).

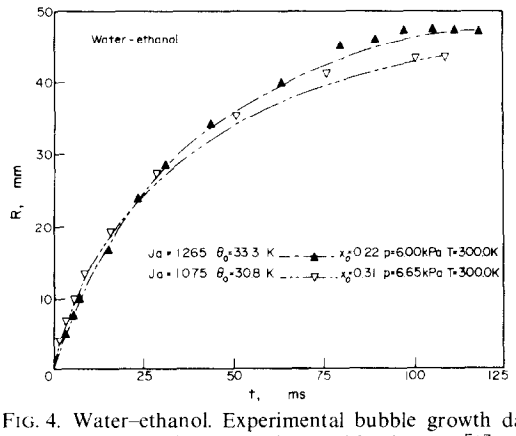

FIG. 4. Water–ethanol. Experimental bubble growth data up to departure in comparison with theory, [1] and equations (1)–(9).

5. EXPERIMENTAL RESULTS AND COMPARISON TO THEORETICAL PREDICTIONS FOR WATER–ETHANOL AND WATER–1-BUTANOL

5.1. *Water–ethanol*

Bubble growth curves. The experimental equivalent bubble radius $R(t)$ (up to departure) is shown for $x_0 = 0$ (water) and $x_0 = 0.10$ (Fig. 3) and for $x_0 = 0.22$ and $x_0 = 0.31$ (Fig. 4). The theoretical curves in Figs. 3 and 4 are derived from the van Stralen *et al.* theory [1], cf. equations (1)–(9) of Sections 3.1 and 3.2.

Initial growth. Obviously, initial bubble growth is determined by the Rayleigh solution (i.e. the bubble is blown up), which is approximately independent of liquid composition in the binary systems investigated.

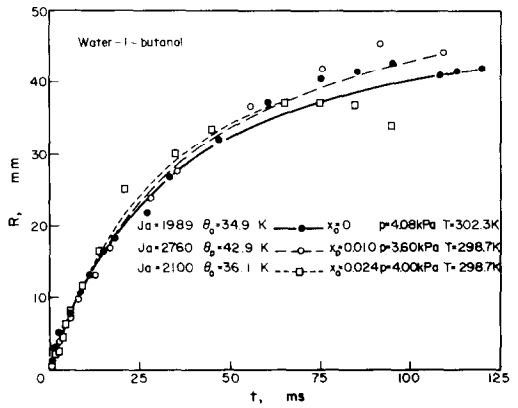

FIG. 5. Water–1-butanol. Experimental bubble growth data up to departure in comparison with theory, [1] and equations (1)–(9).

Advanced growth. Curiously, experimental advanced growth in the investigated mixtures, which should be slowed down due to mass diffusion, is also independent of liquid composition. This effect is attributed to a local depletion of the more volatile component in a liquid layer surrounding the bubble, resulting in $\Delta T \to 0$ (water) due to $G = (x_0 - x)/(y - x) \to 1$, i.e. $y \to x_0$, hence $x_0 \to 0$. Actually, at constant pressure, a minimal value of the ratio $C_{1,m}/C_{1,p} = 0.67$ (in the investigated range of concentrations) occurs at $x_0 = 0.10$. This value is relatively large, hence the showing-down effect of mass diffusion on advanced bubble growth is limited a priori.

5.2. *Water–1-butanol*

The experimental results for this system (Fig. 5) are similar to those for water–ethanol, cf. Section 5.1. In this case also, experimental data are in quantitative agreement with the van Stralen *et al.* model [1]. A minimal $C_{1,m}/C_{1,p} = 0.56$ occurs at $x_0 = 0.015$. In the system water–1-butanol too, an effect of mass diffusion during advanced growth has not been observed. The bubble departure radius decreases slightly with increasing mass fraction of the more volatile component; this is probably due to a decrease in surface tension in this "positive" binary system. The theoretical curve for $x_0 = 0.024$ (Fig. 5) is fitted to the experimental maximum bubble radius, which occurs at $t = 64$ ms. The concerning bubbles in $x_0 = 0.010$ and $x_0 = 0.024$ implode already before departure. This is attributed to the increase in dew point of vapour in these mixtures; condensation occurs if the upper part of the bubble boundary is in contact with slightly superheated liquid of the bulk.

Conclusions. Initial bubble growth is governed by the Rayleigh solution, equation (2), i.e. the bubble is blown up by an excess pressure due to a superheating at the bubble boundary (and of the vapour). The initial

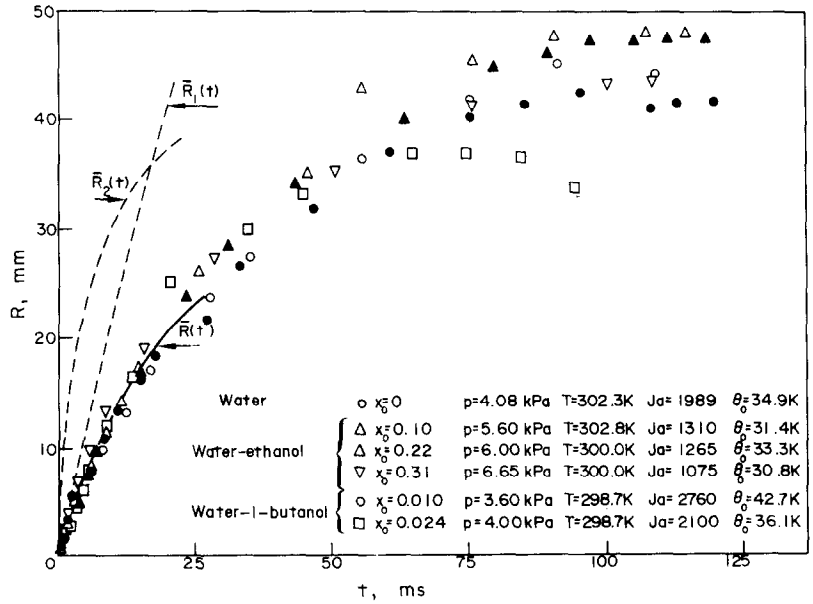

FIG. 6. Water–ethanol and water–1-butanol. Experimental bubble growth data up to departure. Initial growth is mainly governed by R_1, equation (2); R_1, R_2, equation (3), and the resulting R, equation (1), are drawn at average pressure (4.99 kPa), saturation temperature (300.4 K) and wall superheating (34.9 K).

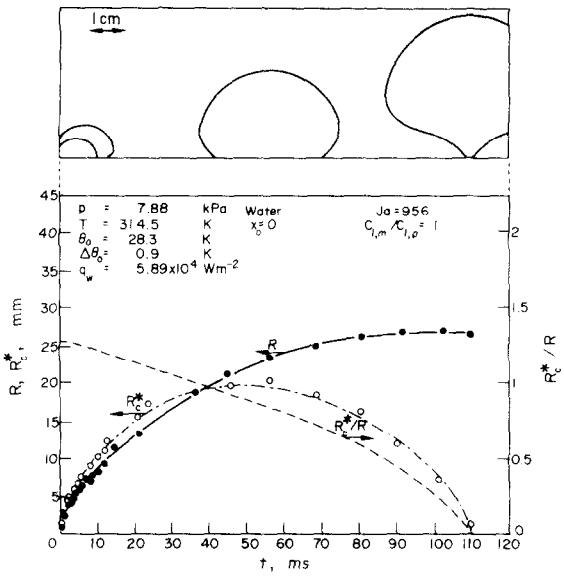

FIG. 7. Water boiling at 7.88 kPa, cf. Fig. 12. Equivalent bubble radius, R, contact radius, R_c^*, and ratio, R_c^*/R, in dependence on time. Corresponding bubble profile and limit of mode of hemispherical growth are shown in the upper drawings.

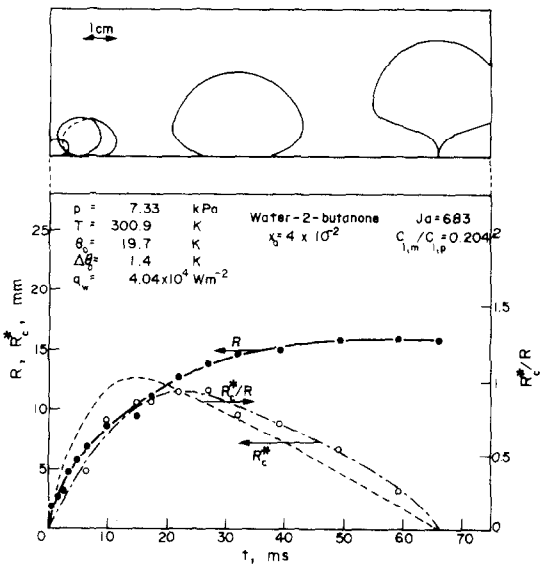

FIG. 9. Water–2-butanone (4 wt% 2-butanone) boiling at 7.33 kPa, cf. Fig. 14. Equivalent bubble radius, R, contact radius, R_c^*, and ratio R_c^*/R, in dependence on time. Corresponding bubble profile is shown in the upper drawings. Initial mode of growth is ellipsoidal.

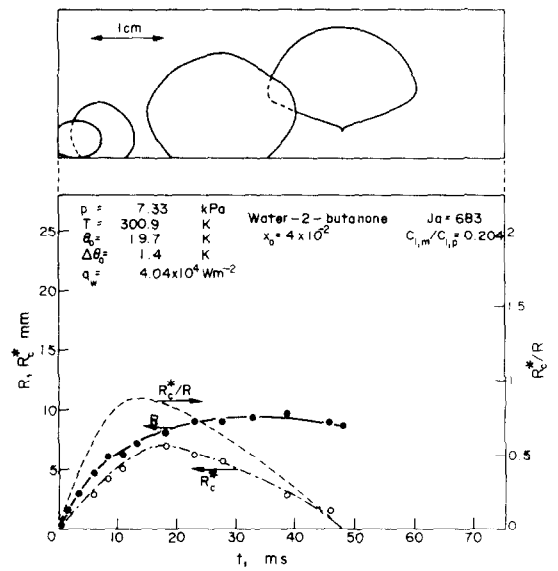

FIG. 8. Water–2-butanone (4 wt% 2-butanone) boiling at 7.33 kPa, cf. Fig. 13. Equivalent bubble radius, R, contact radius R_c^*, and ratio, R_c^*/R, in dependence on time. Corresponding bubble profile is shown in the upper drawings. Initial mode of growth is ellipsoidal.

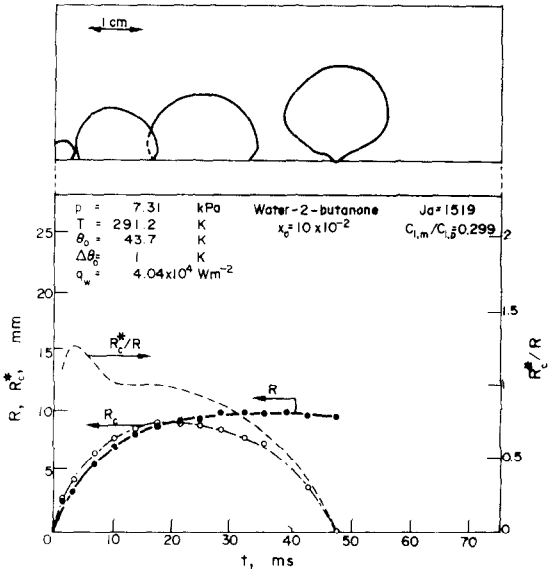

FIG. 10. Water–2-butanone (10 wt% 2-butanone) boiling at 7.31 kPa, cf. Fig. 15. Equivalent bubble radius, R, contact radius, R_c^*, and ratio, R_c^*/R in dependence on time. Corresponding bubble profile is shown in the upper drawings. Initial mode of growth is ellipsoidal.

growth rate is thus approximately independent of liquid composition in case of sufficiently small values of x_0 (Fig. 6). Advanced growth is diffusion-controlled; the expected effect of mass diffusion has not been observed in water–ethanol and in water–1-butanol, probably due to a local depletion of the organic component.

6. EXPERIMENTAL RESULTS AND COMPARISON TO THEORETICAL PREDICTIONS FOR WATER–2-BUTANONE

Bubble growth curves

This system has been investigated more extensively as the relative bubble growth constant $C_{l,m}/C_{l,\rho}$ shows a low minimum value of 0.20 at $x_0 = 0.04$. *A priori*, a strong influence of mass diffusion on advanced bubble growth may be expected to occur in this mixture. Figures 7–11 show the experimental equivalent bubble radius curves $R(t)$ up to departure for various mixtures in the range $x_0 = 0$ (water) to $x_0 = 0.15$. Detailed information on the values of the influential parameters is given in legends at the figures. The simultaneous bubble profile in dependence on time is drawn at the top of the figures. The limitation of the initial mode of hemispherical growth in water (Fig. 7) is denoted by the last picture showing this shape ($t = 5$ ms). In

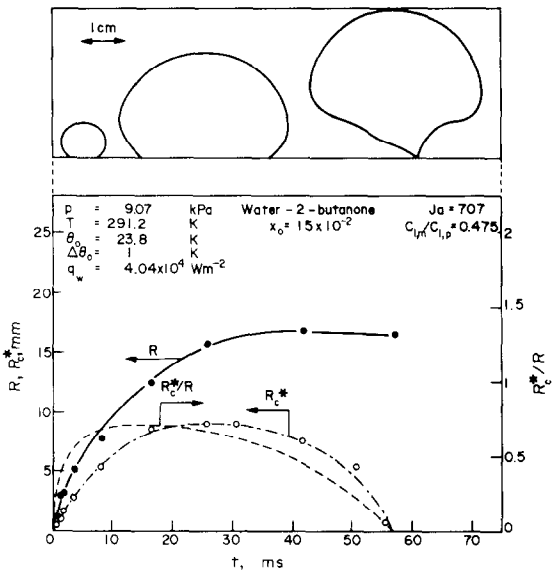

FIG. 11. Water–2-butanone (15 wt% 2-butanone) boiling at 9.07 kPa, cf. Fig. 16. Equivalent bubble radius, R, contact radius, R_c^*, and ratio R_c^*/R, in dependence on time. Corresponding bubble profile is shown in the upper drawings. Initial mode of growth is ellipsoidal.

the investigated mixtures, hemispherical bubble growth has not been observed initially: the bubble has the profile of a rotation ellipsoid.

Initial growth

If the mutual differences in pressure and wall superheating are taken into consideration, it is obvious, that initial growth is governed by the Rayleigh solution, cf. equation (2) and Fig. 6, i.e. initially the bubble is blown up due to an excess pressure.

Advanced growth

Advanced growth is heat and mass diffusion-controlled, bubble growth is slowed down maximally in the range $x_0 = 0.04$ to $x_0 = 0.10$ (Figs. 7–11).

Bubble departure radius

The equivalent departure radius shows a minimum at $x_0 = 0.04$ (Fig. 8), which amounts to approximately 30% of the corresponding value in water (Fig. 7) and to 50% of the value in $x_0 = 0.15$ (Fig. 11). The investigated bubbles in $x_0 = 0.04$ (Figs. 8 and 9) show a difference of a factor of 2 in the departure radius. This is due to a different waiting time before the concerning bubble is generated: the small bubble, which is shown in Fig. 8, has been generated shortly after departure of the larger bubble, shown in Fig. 9. Apparently, an increase in preceeding waiting results in a higher advanced bubble growth rate. The value of the corresponding bubble growth parameter has been increased from $b_m^* = 1.54$ (Fig. 8) to $b_m^* = 1.98$ (Fig. 9); this is attributed to the penetration of heat from the heating surface into the liquid during a larger time interval. This effect is incorporated in the Mikic *et al.* model [8].

Bubble departure time

The bubble departure time decreases gradually from $t_{1,p} = 110$ ms in $x_0 = 0$ (water, Fig. 7) to $t_{1,m} = 56$ ms in $x_0 = 0.15$ (Fig. 11). Probably, this is mainly due to a decrease in surface tension in combination to a gradient in surface tension along the bubble boundary (Marangoni-effect).

Radius of contact area

Figures 7–11 show also the actual radius $R_c^*(t)$ of the contact area between bubble and heating surface.

Obviously, during the *initial hemispherical growth period in water*: $R_c^*/R = 2^{\frac{1}{2}} = 1.26$ (Fig. 7). Afterwards, R_c^*/R decreases approximately linearly with exception of the final period shortly before bubble departure, during which a higher contraction rate of the contact area is shown. $R_c^*(t)$ shows a maximum at the relative time t_c/t_1, which amounts to 0.44 ($x_0 = 0$, water, Fig. 7), 0.37 ($x_0 = 0.04$, Figs. 8 and 9), 0.37 ($x_0 = 0.10$, Fig. 10) and 0.50 ($x_0 = 0.15$, Fig. 11), respectively. The theoretical value for diffusion-controlled bubble growth in water, boiling at a pressure of 7.88 kPa amounts to 0.28, cf. equation (69) of [1] and Table 1 of [2].

Contrarily to the behaviour in water, *in the investigated mixtures* $R_c^*/R \to 0$ as $t \to 0$: the bubble shape is ellipsoidal instead of hemispherical. Consequently, an evaporation layer beneath the bubble is not formed initially. This behaviour is attributed to the Marangoni-effect in "positive" binary systems, cf. Section 4.3 of [1]. The evaporation microlayer is apparently only present during advanced growth, hence equations (2) and (3) are still valid in positive systems.

Bubble oscillations

In some cases (Fig. 7 for water) oscillations in the equivalent bubble radius are observed. These oscillations are due to an interaction of the Rayleigh solution and the diffusion solution and will be treated theoretically in a forthcoming paper by Joosten, Zijl and van Stralen [13]. Bubble oscillations have been observed previously by van Stralen [14].

Comparison with the theory of van Stralen et al. *[1], cf. equations (1)–(9)*

The experimental bubble growth data are in quantitative agreement with theoretical predictions (Figs. 12–16). The numerical value of the bubble growth parameter b^* amounts 0.20 ($x_0 = 0$, water, Fig. 12), 1.54 ($x_0 = 0.04$, Fig. 13), 1.98 ($x_0 = 0.04$, Fig. 14), 0.35 ($x_0 = 0.10$, Fig. 15) and 1.13 ($x_0 = 0.15$, Fig. 16), respectively. The relatively large value in some mixtures are an indication for a local partial depletion of the more volatile component in the liquid surrounding the bubble, cf. Sections 5.1 and 5.2. Nevertheless, the slowing-down effect of mass diffusion on advanced bubble growth is shown clearly for the investigated mixtures in the range $x_0 = 0.04$ to $x_0 = 0.10$.

The evaporation microlayer

The contribution of the evaporation microlayer during the mode of advanced bubble growth in the

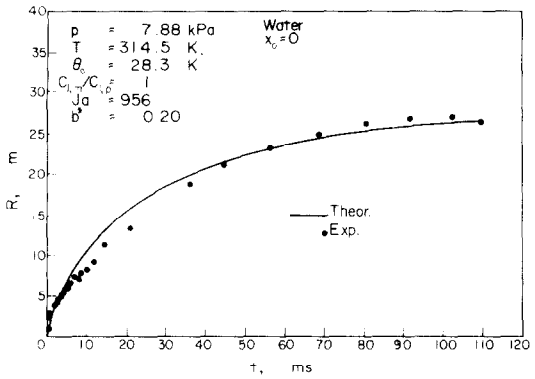

FIG. 12. Water boiling at 7.88 kPa, cf. Fig. 7. Experimental bubble growth data up to departure in comparison with theory, [1] and equations (1)–(9).

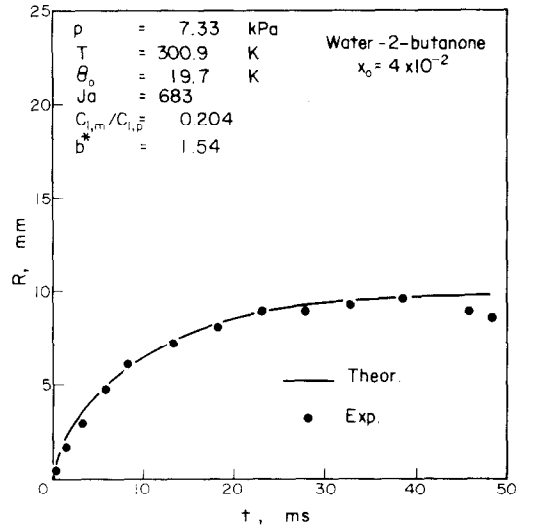

FIG. 13. Water–2-butanone (4 wt% 2-butanone) boiling at 7.33 kPa, cf. Fig. 8. Experimental bubble growth data up to departure in comparison with theory, [1] and equations (1)–(9).

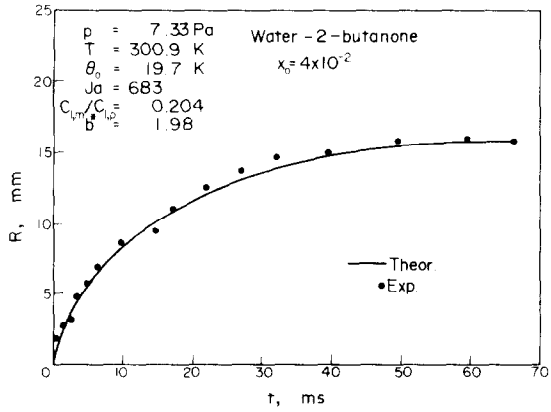

FIG. 14. Water–2-butanone (4 wt% 2-butanone) boiling at 7.33 kPa, cf. Fig. 9. Experimental bubble growth data up to departure in comparison with theory, [1] and equations (1)–(9).

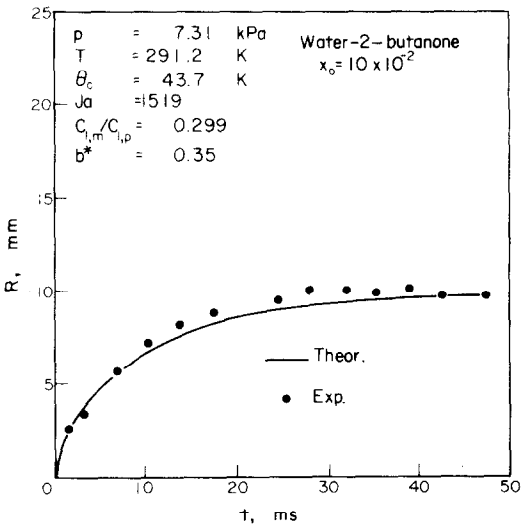

FIG. 15. Water–2-butanone (10 wt% 2-butanone) boiling at 7.31 kPa, cf. Fig. 10. Experimental bubble growth data up to departure in comparison with theory, [1] and equations (1)–(9).

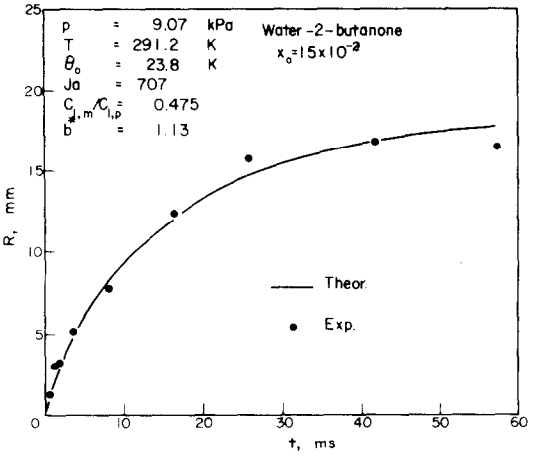

FIG. 16. Water–2-butanone (15 wt% 2-butanone) boiling at 9.07 kPa, cf. Fig. 11. Experimental bubble growth data up to departure in comparison with theory, [1] and equations (1)–(9).

investigated mixtures is relatively small. It follows from equation (3), that the ratio of the contributions to the advanced bubble growth rate due to evaporation microlayer and relaxation microlayer is independent of both time and of initial wall superheating and amounts to: $(C_{1,m}/C_{1,p})(0.191\,Pr^{-\frac{1}{3}}/b^*)$. According to Table 1 of [2], the experimental value of $b_p^* = 0.20$ for bubbles in water boiling at a pressure of 7.88 kPa (Figs. 7 and 12); the corresponding ratio of the microlayer contributions amounts to 0.79. In the investigated mixtures, this ratio is diminished considerably: e.g. for $x_0 = 0.04$ (Figs. 8, 9, 13 and 14) to a value of only 0.02. This value is increased up to 0.21 maximally, if the average b_m^* is reduced from 1.76 to 0.52, cf. the next section on the height of the relaxation microlayer. *Obviously, the contribution of the evaporation microlayer (beneath the bubble) to advanced bubble growth in binary mixtures (with a more volatile component) is small or even*

negligible. This statement holds both at subatmospheric and at elevated pressure as b^* increases with increasing pressure, cf. the values for water in Table 1 of [2].

Maximum height of relaxation microlayer (around the bubble dome)

According to Table 1 of [2], this height, $2b^*R(t_1)$, amounts to approximately 11 mm for bubbles in water at 7.88 kPa (Figs. 7 and 12). In $x_0 = 0.04$ (Figs. 8 and 13) at 7.33 kPa, a value of 37 mm is calculated. A difference between these values (for $x_0 = 0$ and $x_0 = 0.04$) is unsatisfactory from a physical standpoint. If (in the extreme case) the value of 11 mm for water is accepted for the mixture also, i.e. if b_m^* is reduced from 1.76 to 0.52, one has—according to equation (3)—to enlarge the theoretical bubble constant ratio $C_{1,m}/C_{1,p} = 0.20$ (Figs. 8 and 12) to 0.66. This confirms the above-mentioned assumption of the occurrence of a local depletion of the more volatile component in a liquid layer surrounding rapidly growing large vapour bubbles. However, from a physical point of view, it seems to be more reasonable to compare the investigated bubbles in the mixture $x_0 = 0.04$ (Figs. 8, 9, 13 and 14) at 7.33 kPa with bubbles in water boiling at 20.28 kPa, cf. Table 1 and Figs. 4 and 20 of [2], viz. these bubbles have approximately equal departure radii of 12 mm, but the experimental $b_p^* = 1.17$ and the maximal height of the relaxation microlayer amounts to 28 mm. If the latter value is also accepted for the concerning mixture at 7.33 kPa, the ratio $C_{1,m}/C_{1,p}$ increases from 0.20 to 0.26, b_m^* decreases from 1.76 to 1.33, and the relative contribution to advanced bubble growth of the evaporation microlayer in comparison to the relaxation microlayer increases slightly from 0.02 to 0.03. A very limited depletion of the more volatile component is assumed to occur now, and the value (1.33) of b_m^* at 7.33 kPa differs only slightly from the value (1.17) of b_p^* at 20.28 kPa.

Conclusion

The contribution of the evaporation microlayer in binary mixtures (with a more volatile component), in which advanced bubble growth is slowed down considerably due to mass diffusion, it is at least small or even negligible. This statement holds at any pressure, as the evaporation microlayer contribution vanishes both at elevated pressures, cf. [2], and at decreasing pressure, at which Rayleigh bubbles occur [2].

The bubble cycle

The curious bubble cycle, which has been observed previously in water during nucleate boiling at pressures of 2–8 kPa, cf. Section 3.4 and Figs. 12–16 of [2], occurs also in the investigated binary mixtures. In general, directly after departure of a large primary bubble, an initially very rapidly growing thin secondary vapour column is generated on the nucleation site at the heating surface. A comprehensive description and qualitative explanation of this phenomenon has been presented in Section 3.4 of [2].

7. CONCLUSIONS

Experimental bubble growth in the investigated binary systems is in quantitative agreement with the van Stralen *et al.* theory [1]. This model combines the Rayleigh solution (governing isothermal initial growth) with a (heat and mass) diffusion-type solution (governing advanced isobaric growth), which accounts for the contributions to bubble growth due to both the relaxation microlayer (around the bubble dome) and the evaporation microlayer (beneath the bubble). The slowing-down effect of mass diffusion on bubble growth in binary systems (with a more volatile component) occurs only in mixtures with a low relative bubble growth constant $C_{1,m}/C_{1,p}$, e.g. in 4 and 10 wt% 2-butanone in water.

Acknowledgements—One of the authors (R. Cole) was privileged to spend a full year (1971–1972) on sabbatical leave at Eindhoven University. F. J. M. Ramakers, L. J. Bour and M. J. M. Verbruggen carried out experiments and performed the frame by frame analysis of the high speed films. Some of the theoretical curves have been calculated by L. J. Bour using a computer programme.

REFERENCES

1. S. J. D. van Stralen, M. S. Sohal, R. Cole and W. M. Sluyter, Bubble growth rates in pure and binary systems: combined effect of relaxation and evaporation microlayers, *Int. J. Heat Mass Transfer* **18**, 453–467 (1975).
2. S. J. D. van Stralen, R. Cole, W. M. Sluyter and M. S. Sohal, Bubble growth rates in nucleate boiling of water at subatmospheric pressures, *Int. J. Heat Mass Transfer* **18**, 655–669 (1975).
3. R. Cole and S. J. D. van Stralen, Bubble growth rates at low pressures, Preprint "Session on Fundamental Research", in Heat and Mass Transfer, AJChE Annual Meeting, Los Angeles (1975).
4. J. K. Stewart and R. Cole, Bubble growth rates during nucleate boiling at high Jakob numbers, *Int. J. Heat Mass Transfer* **15**, 655–663 (1972).
5. M. G. Cooper and R. M. Vijuk, Bubble growth in nucleate pool boiling, *Proc. 4th Int. Heat Transfer Conf., Paris–Versailles*, Vol. 5, p. B2.1. Elsevier, Amsterdam (1970).
6. W. Zijl, Global collocation approximations of the flow and temperature fields around a gas and a vapour bubble. To be published.
7. H. S. Carslaw and J. C. Jaeger, *Conduction of Heat in Solids*, 2nd edn. Clarendon Press, Oxford (1959).
8. B. B. Mikic, W. M. Rohsenow and P. Griffith, On bubble growth rates, *Int. J. Heat Mass Transfer* **13**, 657–666 (1970).
9. J. C. Chu, R. J. Getty, L. F. Brennecke and R. Paul, *Distillation Equilibrium Data*. Reinhold, New York (1950); J. C. Chu, S. L. Wang, S. L. Levy and R. Paul, *Vapor–Liquid Equilibrium Data*. Edwards, Ann Arbor, Michigan (1956).
10. K. Jellinek, *Lehrbuch der physikalischen Chemie*, Vols. 2–4. Enke, Stuttgart (1928–1933).
11. R. Kubo, H. Ichimura, T. Usui and N. Hashitsume, *Thermodynamics, an Advanced Course with Problems and Solutions*. North-Holland, Amsterdam (1968).
12. B. F. Dodge, *Chemical Engineering Thermodynamics*, 1st edn. McGraw-Hill, New York (1944).
13. J. G. H. Joosten, W. Zijl and S. J. D. van Stralen, Growth of a vapour bubble in combined gravitational and nonuniform temperature fields. To be published.
14. S. J. D. van Stralen, Bubble growth rates in boiling binary mixtures, *Br. Chem. Engng* **12**, 390–394 (1967).
15. S. J. D. van Stralen, The growth rate of vapour bubbles in superheated pure liquids and binary mixtures, Parts

I–II, *Int. J. Heat Mass Transfer* **11**, 1467–1490, 1491–1512 (1968).
16. S. J. D. van Stralen, The mechanism of nucleate boiling in pure liquids and in binary mixtures, Parts I–IV, *Int. J. Heat Mass Transfer* **9**, 995–1020, 1021–1046 (1966); **10**, 1469–1484, 1485–1498 (1967).
17. S. J. D. van Stralen, The boiling paradox in binary liquid mixtures, *Chem. Engng Sci.* **25**, 149–171 (1970).
18. S. J. D. van Stralen, Kookverschijnselen, Part 6, Het mechanisme van kernkoken in unaire en binaire systemen, (I), Fysische grondslagen, *Polytechn. tijdschr.*, ed. *Procestechniek* **30**, 249–258 (1975); (II), Theorie en experiment, *Polytechn. tijdschr.*, ed. *Procestechniek* **30**, 278–289 (1975). (In Dutch.)
19. S. J. D. van Stralen, Warmteoverdracht aan kokende binaire vloeistofmengsels, Ph.D. thesis, University of Groningen, Netherlands (1959); *Meded. Landb. Hoogesch. Wageningen* **59** (6), 1–84 (1959). (In Dutch with English summary and captions.)
20. S. J. D. van Stralen, Heat transfer to boiling binary liquid mixtures, Parts I–IV, *Br. Chem. Engng* **4**, 8–17, 78–82 (1959); **6**, 834–840 (1961); **7**, 90–97 (1962).

APPENDIX

Expressions for $\Delta T/G$, *the Relative Bubble Growth Constant and the Relative Nucleate Boiling Peak Flux in Binary Systems*

In an improved version of the relaxation microlayer theory for the mechanism of nucleate boiling [16, 17], van Stralen [18] has shown, that for ideal binary systems (or more generally for $x_0 \ll 1$) at constant pressure:

$$T_p - T_m \approx -x_0\left(\frac{dT}{dx}\right)_{x=x_0}, \tag{11}$$

and

$$\frac{\Delta T}{G} \approx -x_0(K-1)\left(\frac{dT}{dx}\right)_{x=x_0}. \tag{12}$$

Hence, as an approximation:

$$\frac{\Delta T}{G} = (K-1)(T_p - T_m) \tag{13}$$

It follows by combining Raoult's law and the Clapeyron equation (10), that (at constant pressure):

$$T_p - T_m = \frac{T_p}{\rho_2 l}p(y-x) = \frac{T_p}{\rho_2 l}p(K-1)x. \tag{14}$$

Substitution of (14) into (13) yields an expression, which relates $\Delta T/G$ to the fraction x at the bubble boundary:

$$\frac{\Delta T}{G} = \frac{T_p}{\rho_2 l}(K-1)^2 px. \tag{15}$$

According to the ideal gas law, $\rho_2 \sim p$ at low pressures. Consequently (*at constant liquid composition*), *the increase* ΔT *in dew point of vapour (divided by the vaporized mass fraction* G*) is then approximately independent of pressure.* Equation (15) expresses $\Delta T/G$ into material constants and is useful to derive $\Delta T/G$ for binary systems at sub-atmospheric pressures, especially if equilibrium data are not known in literature. As an approximation for this case, one can start from the values of $\Delta T/G$, which are derived (e.g. graphically) from the equilibrium diagram at atmospheric pressure. This procedure has been used in case of the systems water–1-butanol and water–2-butanone, cf. Sections 5.1 and 6, to evaluate the value of the bubble growth constant $C_{1,m}$, equation (4), for the investigated mixtures. It follows from equations (4), (5) and (15), that

$$\frac{C_{1,p}}{C_{1,m}} = 1 + \left(\frac{a}{D}\right)^{\frac{1}{2}}\frac{cpT_p}{\rho_2 l^2}(K-1)^2 x \tag{16}$$

i.e. the relative bubble growth constant (for asymptotic diffusion-controlled growth) in mixtures, $C_{1,m}/C_{1,p}$, is also expressed into material constants. According to equation (14), this is also the case for the relative peak flux in nucleate boiling of mixtures, cf. the van Stralen relaxation microlayer theory for the mechanism of nucleate boiling [16–18]:

$$\frac{q_{w,m,\max}}{q_{w,p,\max}} = 1.89\left(1 + \frac{T_p - T_m}{\Theta_{0,p,\max}}\right) = 1.89\left\{1 + \frac{T_p}{\Theta_{0,p,\max}}\frac{p}{\rho_2 l}(K-1)x\right\}. \tag{17}$$

In case of $G = (x_0 - x)/(y - x) \ll 1$, one may replace x in equations (15)–(17) by the known x_0, which applies to the original liquid composition. *Both the concentration of minimal bubble growth constant and the coinciding concentration of maximal relative peak flux in nucleate boiling of "positive" binary systems (with a more volatile component) are thus approximately independent of pressure.* These quantities are governed by the factors $(K-1)x \approx y$, and $(K-1)^2 x \approx y^2/x = Ky$. In case of non-ideal binary systems both $(K-1)x = 0$ and $(K-1)^2 x = 0$ for $x = 0$ (pure liquids). At the azeotrope, $y = x$ (i.e. $K = 1$), hence these functions equal zero then also. At an intermediate concentration of the more volatile component, both functions show a maximum, coinciding with a maximal $\Delta T/G$, a maximal $q_{w,m,\max}$ and a minimal $C_{1,m}$, cf. [17, 18]. The independence of pressure (in a limited range) has been shown previously by van Stralen [19, 20].

It follows from equations (16) and (17) that the minimal $C_{1,m}$ decreases and the maximal $q_{w,m,\max}$ increases as K increases, cf. the behaviour of the aliphatic alcohols in water [19, 20]. Obviously, in case of non-ideal binary systems, equations (13)–(17) are approximations, which are more accurately as $x_0 \to 0$.

ERRATA ON PREVIOUS PAPERS [1, 2]

(i) The procedure to derive an expression for the total bubble radius, cf. Section 5.1 of [1], results in a superposition of separate radii due to relaxation and evaporation microlayers, respectively. In principle, Cooper, cf. reference [8] of [1] and Van Ouwerkerk, cf. references [10, 11] of [1] used a similar procedure in the case of initially uniform liquid superheating. As a consequence, the last paragraph: "A serious ... Section 5.1" of Section 3.1.3 of [1] has to be cancelled.

(ii) The sixth line from top: "i.e. only ... volume", page 457 of [1] is incorrect and has to be cancelled. Second line from bottom, page 460 of [1]: "resistances" has to be replaced by "conductances".

(iii) In Section 5.1 of [1], with exception of equation (58), the (equivalent spherical) bubble radius, R, should be replaced by R^*, the radius of the hemispherical bubble. Also, the factor $2^{\frac{1}{2}}$ in the denominator in the RHS of equation (56) of [1] has to be omitted.

(iv) Table 1 of [2]: at a pressure of 2.04 kPa, the value of the bubble growth parameter b^* (2.547) has to be replaced by 0.675, and the value of b (2.684) by 0.812. The correct values are calculated using the complete equation (63) of [1]: the original incorrect values are derived by neglecting the superheating $\Delta\theta_0$ of the bulk liquid in the RHS of this equation.

Consequently, the first footnote, (*), to Table 1 of [2] has to be replaced by the following: "The ratio of evaporation to relaxation microlayer contribution to bubble growth amounts to 0.204 at a pressure of 2.04 kPa. This relatively low ratio is due to the dominating influence of the Rayleigh solution on bubble growth at low pressures. In this case, the evaporation microlayer hardly contributes to bubble growth as the initial temperature drop across this layer equals zero, cf. equations (62) and (65) of [1]. During the mode of initial isothermal growth, equation (21) of [1] reduces to an identity".

VITESSE DE CROISSANCE DES BULLES EN EBULLITION NUCLEEE DES SYSTEMES BINAIRES AQUEUX AUX PRESSIONS SUBATMOSPHERIQUES

Résumé—On a étudié expérimentalement le développement des bulles de vapeur dans les systèmes binaires suivants qui comprennent un constituant organique plus volatil: eau–éthanol (jusqu'à 31% d'éthanol, à des pressions comprises entre 4,08 et 6,65 kPa, le nombre de Jakob variant de 1989 à 1075), eau–1-butanol (jusqu'à 2,4% de 1-butanol, à des pressions comprises entre 3,60 et 4,08 kPa, le nombre de Jakob variant de 2760 à 1989), et eau–2-butanone (jusqu'à 15% de 2-butanone, à des pressions comprises entre 7,31 et 9,07 kPa, le nombre de Jakob variant de 1519 à 683).

La croissance des bulles observée expérimentalement est en accord quantitatif avec la théorie de Van Stralen, Sohal, Cole et Sluyter [1], combinant une solution de Rayleigh qui prévaut initialement avec une solution de type diffusion (chaleur et masse) qui décrit les contributions de la microcouche de relaxation (autour du dome de la bulle) et la microcouche d'évaporation (au dessous de la bulle) au développement ultérieur des bulles.

L'effet modérateur de la diffusion massique sur le développement avancé des bulles dans les mélanges ne se produit que pour le système eau–2-butanone. La contribution de la microcouche d'évaporation est négligeable (à toute pression) pour des mélanges à faible concentration du composant le plus volatil, dans lequel la diffusion de masse limite considérablement l'avancement de la croissance des bulles.

WACHSTUMSGESCHWINDIGKEIT VON DAMPFBLASEN BEIM BLASENSIEDEN VON WÄSSRIGEN BINÄR-SYSTEMEN BEI DRÜCKEN UNTERHALB DES ATMOSPHÄRENDRUCKES

Zusammenfassung—Die Wachstumsrate von Dampfblasen wurde experimentell untersucht in folgendem binären System mit einer leichtflüchtigen organischen Komponente: Wasser–Aethanol (bis zu 31 Gewichtsprozent Aethanol, bei Drücken zwischen 4,08 und 6,65 kPa, einer Jakob–Zahl zwischen 1989 und 1075), Wasser–1-butanol (bis zu 2,4 Gewichtsprozent 1-Butanol, bei Drücken zwischen 3,60 und 4,08 kPa, einer Jakob–Zahl zwischen 2760 und 1989), und Wasser–2-butanon (bis zu 15 Gewichtsprozent 2-butanon, bei Drücken zwischen 7,31 und 9,07 kPa, einer Jakob–Zahl zwischen 1519 und 683).

Das experimentelle Blasenwachstum ist in quantitativer Übereinstimmung mit der Theorie nach van Stralen, Sohal, Cole und Sluyter [1]. Diese Theorie kombiniert die anfänglich dominierende Rayleigh Lösung mit einer (Wärme und Stoff) Diffusions-Lösung für die Beiträge des fortgeschrittenen Blasenwachstums infolge der Relaxationsmikroschicht (um die Blase) und der Verdampfungsmikroschicht (unter der Blase).

Der Verzögerungseffekt der Stoffdiffusion bei forgeschrittenem Blasenwachstum in Gemischen zeigt sich nur im System Wasser–2-butanon. Der Beitrag der Verdampfungsmikroschicht ist vernachlässigbar (bei jedem Druck) für Gemische mit einer geringen Konzentration der leichter flüchtigen Komponente, wobei die Stoffdiffusion das fortgeschrittene Wachstum erheblich begrenzt.

СКОРОСТИ РОСТА ПУЗЫРЬКОВ ПРИ ПУЗЫРЬКОВОМ КИПЕНИИ В ВОДНЫХ БИНАРНЫХ СИСТЕМАХ ПРИ ДАВЛЕНИИ НИЖЕ АТМОСФЕРНОГО

Аннотация — Проведено экспериментальное исследование скорости роста пузырьков пара в следующих бинарных системах с более летучим органическим компонентом: вода-этанол (до 31 водн. % этанола, при давлении от 4.08 до 6.65 кн/м² и числе Якоба от 1989 до 1075); вода-1-бутанол (до 2.4 водн. % 1-бутанола, при давлении от 3.60 до 4.08 кн/м² и числе Якоба от 2760 до 1989); и вода-2-бутанол (до 15 водн. % 2-бутанола при давлении от 7.31 до 9.07 кн/м² и числе Якоба от 1519 до 683).

Экспериментальные данные по скорости роста пузырька находятся в количественном соответствии с теорией Ван Штралена, Сохаля, Коула и Слютера [1], предлагающей систему из уравнения для первоначального доминирующего числа Рэлея и уравнения диффузии (тепла и массы) для определения влияния релаксационного микрослоя (вокруг купола пузырька) и испаряющегося микрослоя (под пузырьком).

Замедляние скорости роста пузырьков под влиянием диффузии массы в смесях проявляется только в системе вода-2-бутанола. Влияние испаряющегося микрослоя незначительно (при любом давлении) в смесях с низкой концентрацией более летучего компонента, диффузия массы которого значительно ограничивает рост пузырьков.